JOURNAL OF VIROLOGY, Apr. 2003, p. 3950–3961 Vol. 77, No. 7
0022-538X/03/$08.00+0 DOI: 10.1128/JVI.77.7.3950–3961.2003

Hepatitis C Virus NS3 ATPases/Helicases from Different Genotypes Exhibit Variations in Enzymatic Properties

Angela M. I. Lam, David Keeney, Patrick Q. Eckert, and David N. Frick*

Department of Biochemistry and Molecular Biology, New York Medical College, Valhalla, New York 10595

Received 23 July 2002/Accepted 30 December 2002

The NS3 ATPase/helicase was isolated and characterized from three different infectious clones of hepatitis C virus (HCV). One helicase was from a genotype that normally responds to therapy (Hel-2a), and the other two were from more resistant genotypes, 1a (Hel-1a) and 1b (Hel-1b). Although the differences among these helicases are generally minor, all three enzymes have distinct properties. Hel-1a is less selective for nucleoside triphosphates, Hel-1b hydrolyzes nucleoside triphosphates less rapidly, and Hel-2a unwinds DNA more rapidly and binds DNA more tightly than the other two enzymes. Unlike related proteins, different nucleic acid sequences stimulate ATP hydrolysis by HCV helicase at different maximum rates and with different apparent efficiencies. This nucleic acid stimulation profile is conserved among the enzymes, but it does not result entirely from differential DNA-binding affinities. Although the amino acid sequences of the three proteins differ by up to 15%, one variant amino acid that is critical for helicase action was identified. NS3 residue 450 is a threonine in Hel-1a and Hel-1b and is an isoleucine in Hel-2a. A mutant Hel-1a with an isoleucine substituted for threonine 450 unwinds DNA more rapidly and binds DNA more tightly than the parent protein.

The hepatitis C virus (HCV) evolves so rapidly that, in individual patients infected with certain genotypes, HCV exists as a heterogeneous population of quasispecies. Both viral genotype and quasispecies diversity influence disease severity and treatment response (reviewed in references 9 and 45). Patients infected with genotype 1 often do not respond to antiviral therapy, whereas patients with other genotypes respond more favorably (25). The kinetics of viral load decreases after the initiation of interferon therapy suggested a high free-virion clearance rate, a low rate of virus production in infected cells, and a high rate of infected-cell death in patients infected with genotype 2 relative to those in patients infected with genotype 1 (28). Strains that more rapidly evolve into diverse quasispecies more readily evade the host immune system, leading to chronic hepatitis (10), and respond less well to therapeutic intervention (11). Exactly how HCV genetic variation leads to these clinically important viral phenotypes is still largely a mystery, however. This comparative study was therefore initiated to define the impact of genetic variation on the activity of one of the best characterized HCV proteins, the NS3 helicase.

HCV is a positive-sense, single-stranded RNA (ssRNA), and as such, when it enters a cell, HCV genomic RNA is translated into a peptide over 3,000 amino acids long from a single open reading frame. Both the host and viral proteases process the HCV polyprotein into three structural proteins (core, E1, and E2) and seven nonstructural proteins (p7, NS2, NS3, NS4A, NS4B, NS5A, and NS5B). Most studies dealing with the impact of genetic variation on the HCV life cycle have focused on linking heterogeneity in NS5A (7) and E2 (38) with the treatment response, but their conclusions remain controversial. Some, but not all, of these studies demonstrate that variability in these regions correlates with resistance to various treatments. However, no molecular mechanisms have been elucidated, in part, because neither E2 nor NS5A has clearly defined biological functions. Little is known about the impact of genetic variations on the activities of HCV proteins with well-characterized activities, such as the NS5B polymerase, or about that of the NS3 helicase/protease. The helicase was chosen for this study because it has a clear biological relevance and can be relatively easily expressed and purified as a recombinant protein.

The HCV helicase is part of the NS3 protein, which has two separate independent functional domains. The other NS3 domain contains an essential serine protease that acts to cleave the NS3-to-NS5B region of the HCV polyprotein. The HCV helicase unwinds duplex RNAs that are formed during the viral RNA replication process. Curiously, the HCV helicase unwinds DNA more effectively than RNA (29) even though there is no known DNA intermediate in the HCV life cycle. Several crystal structures (4, 18, 44) and mechanistic studies (20, 21, 23, 26, 29, 32, 33) have helped reveal that the HCV helicase couples energy derived from ATP hydrolysis with the translocation of the protein. The enzyme moves like a molecular motor along one nucleic acid (NA) strand in a 3′-to-5′ direction and, in the process, displaces the cDNA (or RNA) strand. All of the studies described above have focused exclusively on helicases derived from genotype 1a or 1b. None have examined the activity of the helicase derived from other genotypes.

Many previous studies of the HCV helicase report somewhat different results. The discrepancies may be due to differences in assay conditions, expression systems, purification procedures, or genetic variations. A rigorous comparison of the HCV helicase enzymes obtained from different viral isolates has not been reported. However, single amino acid substitutions in the HCV helicase have been repeatedly shown to influence its activity not only in vitro (22, 31, 37) but also in

* Corresponding author. Mailing address: Department of Biochemistry and Molecular Biology, New York Medical College, Valhalla, NY 10595. Phone: (914) 594-4190. Fax: (914) 594-4058. E-mail: David_Frick@NYMC.edu.

TABLE 1. Oligonucleotide sequences

Oligonucleotide	Sequence
1a-*Nhe*I	GCGCGCGCTAGCGTGGACTTTATCCCTGTGGAGA
1a-*Bam*HI	GCGCGCGGATCCCGGGTGCTCGTGACGACCTCCAG
1b-*Nhe*I	GCGCGCGCTAGCGTGGACTTCATACCCGTTGAGTCT
1b-*Eco*RI	GCGCGCGAATTCGGGGTGCTAGTGACGACCTCCAG
2a-*Nhe*I	GCGCGCGCTAGCATAGATTTCATCCCCGTTGAGA
2a-*Bam*HI	GCGCGCGGATCCCGTGTGCTGGTCATGACCTCAAG
T450I sense	CTTTACCATTGAGACAACCATACTCCCCCAGGATGCTGTC
T450I antisense	GACAGCATCCTGGGGGAGTATGGTTGTCTCAATGGTAAAG
dU18	UUUUUUUUUUUUUUUUUU
dT18	TTTTTTTTTTTTTTTTTT
dC18	CCCCCCCCCCCCCCCCCC
dA18	AAAAAAAAAAAAAAAAAA
dCT9	CTCTCTCTCTCTCTCTCT
dGA9	GAGAGAGAGAGAGAGAGA
dAT9	ATATATATATATATATAT
dGC9	GCGCGCGCGCGCGCGCGC
5′C	CCCCCCCCCGCGCGCGCGCGCGCGCGC
3′C	GCGCGCGCGCGCGCGCGCCCCCCCCCC
DNA, RNA, (release strand)	GCCTCGCTGCCGTCGCCA
3′ DNA, (template strand)	TGGCGACGGCAGCGAGGCTTTTTTTTTTTTTTTTTTT
3′ RNA, (template strand)	TGGCGACGGCAGCGAGGCUUUUUUUUUUUUUUUUUU

vivo and by using replicons. Adaptive mutations that allow HCV subgenomic replicons to replicate more efficiently in cell culture accumulate in the helicase (19, 24). Numerous mutations also arise in NS3 during treatment, possibly due to immune selection (39). Likewise, in chimpanzees infected with HCV, mutations that arise in the NS3 helicase allow the virus to escape the effects of cytotoxic T lymphocytes in the liver (8, 40).

In this study, helicases from the infectious clones of the three most common genotypes in North America (1a, 1b, and 2a) were expressed in identical systems, purified, and characterized. The goal was to better understand the molecular consequences of HCV genetic variability and to further define the conserved targets for antiviral agents. Two of the helicases were derived from genotypes that normally do not respond to therapy (genotypes 1a and 1b), and a third was taken from a genotype that normally responds to therapy (genotype 2a). About 15% of the amino acids varied among the genotypes. Most of the basic properties of the helicase were conserved, but there were numerous apparent differences among the proteins. Most importantly, though, the helicase from genotype 2a bound DNA more tightly and unwound it more efficiently than the helicase isolated from either genotype 1b or 1a. A variant residue that contacts the DNA backbone was identified, and mutation of this residue appeared to account for some of these observed differences. The data show that natural genetic variation outside the well-known conserved motifs (13) affects helicase activity and possibly viral replication rates.

MATERIALS AND METHODS

Materials. RNase-free reagents were purchased from Ambion, Inc. (Austin, Tex.). Nucleotides and NAs were treated with RNAsecure reagent (Ambion) according to the manufacturer's instructions. RNA homopolymers were purchased from Sigma, and their concentrations were determined from their extinction coefficients. DNA oligonucleotides were purchased from Integrated DNA Technologies (Coralville, Iowa), and their concentrations were determined from the extinction coefficients provided by their manufacturer.

Genetic constructs. A set of plasmids was constructed to express the various HCV helicases in *Escherichia coli.* HCV cDNA encoding the NS3 protein (amino acids 1193 to 1659 of the polyprotein encoded by genotype 1a or 1b; amino acids 1197 to 1663 of the genotype 2a polyprotein) was inserted in the multiple cloning site of vector pET24a (Novagen). PCR was used to amplify the DNA in separate reactions from three infectious DNA clones of genotype 1a (pCV-H77c [42]), genotype 1b (pJ4L6S [43]), and genotype 2a (pHC-J6CF [41]). Plasmids pCV-H77c, pJ4L6S, and pJ6CF were generous gifts from Jens Bukh (National Institutes of Health). The primers used to amplify and attach 5′ and 3′ restriction sites to helicase cDNA are listed in Table 1. After amplification, DNA containing each helicase was digested with the appropriate restriction enzymes, whose sites are encoded by each primer set, and then purified and ligated into similarly treated vector DNA. The resulting plasmids were sequenced and designated p24Hel-1a, p24Hel-1b, and p24Hel-2a, respectively. In each case, the recombinant helicases were placed under the control of a T7(*lac*) promoter. For expression, the plasmids were used to transform strain BL21(DE3), which contains T7 polymerase under the control of a *lac* promoter. Strains harboring p24Hel plasmids express their respective recombinant HCV helicases with an additional Met, Ala, and Ser at their N terminus and the 20-amino-acid-long sequence PNSSSVDKLAAALEHHHHHH fused to their C terminus. The recombinant proteins were designated Hel-1a, Hel-1b, and Hel-2a.

Threonine 450 of Hel-1a was modified to isoleucine by using a QuikChange site-directed mutagenesis kit (Stratagene) according to the manufacturer's protocol. Two internal mutagenic primers, T450I sense and T450I antisense (Table 1), were employed to incorporate the substitution. Alterations were confirmed by DNA sequencing. Mutant plasmids were transformed into BL21(DE3) cells, and the recombinant protein was expressed and purified as described below.

Protein purification. The same purification scheme described below was used to purify each helicase. Briefly, BL21(DE3) cells (typically 1-liter cultures) harboring each plasmid were grown to an absorbance at 600 nm (A_{600}) of 0.5 and induced with 1 mM isopropyl-β-D-thiogalactopyranoside. After 3 h, cells were harvested by centrifugation, washed in Tris-buffered saline (pH 7.5), and resuspended in 10 ml of 50 mM HEPES (pH 8)–300 mM NaCl–1 mM dithiothreitol (DTT)–10 mM imidazole (buffer A). Cells were lysed by two passes through a French press, and the extract was cleared by centrifugation at 25,000 × *g* (fraction I). Fraction I was loaded onto a 5-ml Ni-nitrilotriacetic acid column (Novagen) previously charged with $NiSO_4$ and equilibrated in buffer A. The column was washed and eluted with buffer A containing a gradient of imidazole from 10 to 300 mM. Fractions containing helicase were combined (fraction II). $(NH_4)_2SO_4$ was added to 60% saturation to fraction II, and the precipitate was dissolved in 1 ml of 50 mM Tris (pH 7.5)–1 mM EDTA–1 mM DTT (buffer B) (fraction III). Fraction III was loaded onto a 100-ml Sephacryl S-200 high-resolution gel filtration column, which was equilibrated and eluted with buffer B, and fractions containing helicase were pooled (fraction IV). Fraction IV was loaded onto a 2-ml DEAE Sepharose column and eluted with an NaCl gradient from 10 to 500 mM. Combined fractions were dialyzed into buffer B containing 50% glycerol for storage (fraction V). Protein concentrations were determined by using A_{280} with the following extinction coefficients calculated from the Trp,

Tyr, and Phe content of each protein: Hel-1a, 42.2 mM^{-1} cm^{-1}; Hel-1b, 42.4 mM^{-1} cm^{-1}; Hel-2a, 48.3 mM^{-1} cm^{-1}.

NTPase assays. Reactions were run at 37°C in 50 mM Tris-Cl (pH 7.5)–10 mM $MgCl_2$–nucleoside triphosphate (NTP)–helicase at the indicated concentrations and terminated with the addition of 0.1 ml of 16% Norit in 5% trichloroacetic acid. After centrifugation at 16,000 × *g* for 10 min, phosphate in the supernatant was measured either by scintillation counting (if [γ-^{32}P]ATP was used as a substrate) or by a colorimetric assay (12). In the colorimetric assay, phosphate-containing solutions (up to 300 μl) were added to 700 μl of freshly prepared 6:1 mixture of 0.42% ammonium molybdate in 1 N H_2SO_4–10% ascorbic acid and incubated for 20 min at 42°C. In this assay, 50 nmol of phosphate yielded an A_{780} of 1.0. Both the radioactive and colorimetric phosphate assays yielded identical results. Data were fit to equation 1 by nonlinear least-square analysis using the Prism program (version 3.02 for Windows; GraphPad Software, San Diego, Calif.).

$$\frac{v}{[E]_T} = \frac{k_{cat}[ATP]}{K_m + [ATP]} \quad (1)$$

Equation 2 was used to determine the k_{cat} in the presence of saturating amounts of NAs and the constant K_{NA}, which defines the amount of NA required to stimulate a half-maximal rate of NTP hydrolysis. $[E]_T$ is the total enzyme concentration.

$$\frac{v}{[E]_T} = \frac{k_{cat}[NA]}{K_{NA} + [NA]} \quad (2)$$

In competition experiments, K_i values were determined from equation 3 by measuring [γ-^{32}P]ATP hydrolysis in the presence and absence of unlabeled NTPs.

$$\frac{v_i}{v_o} = \frac{K_m + [ATP]}{K_m\left(1 + \frac{[I]}{K_i}\right) + [ATP]} \quad (3)$$

In equation 3, [I] is the concentration of unlabeled NTP. The initial velocity in the presence of inhibitor (unlabeled NTP) is v_i, and v_o is the velocity in the presence of ATP only.

Gel shift assays. DNA was labeled with T4 polynucleotide kinase with [γ-^{32}P]ATP and purified from free ATP by using a Sephadex G-25 column. Oligonucleotide concentrations were determined by measuring A_{280}. Binding reactions contained 50 mM Tris (pH 7.5), 10 mM $MgCl_2$, labeled oligonucleotide, and helicase at the indicated concentrations. After 10 min at room temperature, 2 μl of tracking dye (0.25% bromophenol blue, 0.25% xylene cyanol FF, 40% sucrose) was added and the samples were loaded on a 12% native Tris-borate-EDTA (TBE) polyacrylamide gel. After electrophoresis, the gel was dried and analyzed with a Molecular Dynamics Storm 860 PhosphorImager to determine the ratio of bound to free DNA. These ratios were used to calculate the concentrations of bound and free DNA in the original reaction from the total DNA in the reaction.

Fluorimetric titration assays. The quenching of the intrinsic protein fluorescence upon formation of the enzyme-NA (E · NA) complex was monitored as described previously (21, 33). Aliquots of DNA were added to the NS3 helicase (100 nM) in 1 ml of reaction buffer (50 mM morpholinepropanesulfonic acid (MOPS) · NaOH [pH 7.0], 5 mM $MgCl_2$, 5 mM DTT, 0.1% Tween 20) at room temperature. Fluorescence was measured by exciting the sample at 280 nm and reading the emission at 340 nm with a Hyper RF fluorimeter (Shimadzu). Excitation and emission slit widths were set to 3 and 10 nm, respectively. A blank titration in which an equivalent volume of buffer was added to the enzyme was included to correct for the drift in the fluorescence signal. All fluorescence data were corrected for sample dilution and inner-filter effects according to equation 4

$$F_c = F\frac{(V_o + V_i)}{V_o} \times 10^{A_{280}/2} \quad (4)$$

where F_c is the corrected fluorescence, F is the observed fluorescence, v_o is the initial sample volume, and v_i is the total volume of titrant added.

The fractional fluorescence F_{NA} remaining was calculated by dividing F_c by the initial fluorescence value of the protein in the absence of NA. F_{NA} was fit to the total concentration of added NA ($[NA]_T$) by using equation 5

$$F_{NA} = 1 - \Delta F_{MAX}\frac{(K_D + [NA]_T + [E]_T) - \sqrt{(K_D + [NA]_T + [E]_T)^2 + 4[NA]_T[E]_T}}{2[E]_T} \quad (5)$$

in which F_{MAX} is the fractional fluorescence resulting from the total conversion of E to E · NA and K_D is the dissociation constant of E for NA.

DNA helicase assays. HCV helicase assays were performed by measuring the dissociation of duplex DNA under single-turnover conditions as previously described (29). The dissociation of a labeled release strand from a template strand (Table 1) was monitored by gel electrophoresis. To prepare the radiolabeled release strand, [γ-^{32}P]ATP was incorporated in the 5′ end of the release strand with polynucleotide kinase according to the manufacturer's procedure (Roche, Indianapolis, Ind.). To anneal the oligonucleotides, equal concentrations of each appropriate oligonucleotide were mixed in 10 mM Tris (pH 7.5), heated to 90°C, and cooled to room temperature over several hours.

Assays were carried out under single-turnover conditions to measure an observed first-order rate constant, or k_{obs}, of DNA unwinding. HCV helicase (280 nM) and DNA substrate (1 nM) were preincubated in reaction buffer (10 mM Tris [pH 7.0], 5 mM $MgCl_2$) for 10 min at 37°C before initiation by adding 5 mM ATP and trap DNA (3 μM). Unlabeled release strand served to trap the enzyme after it dissociated from the substrate. The trap also prevented unwound DNA from reannealing back to the template DNA. After various times, the reactions were terminated by the addition of stopping buffer (0.25% bromophenol blue, 0.25% xylene cyanol FF, 30% glycerol, 200 mM EDTA, 2% sodium dodecyl sulfate) and separated on a 12% native polyacryamide gel. After 30 min at 200 V, the gel was dried and exposed on a phosphorimager screen. The intensity of the annealed and unwound products was subsequently visualized with a PhosphorImager and quantified by using the ImageQuant software from Molecular Dynamics.

To determine the rate of DNA unwinding, data collected at the various time points during the unwinding assays were fit to equation 6

$$\%U(t) = A_{MAX}(1 - e^{-k_{obs}t}) \quad (6)$$

where $\%U(t)$ is the percentage of duplex unwound at time t. Reaction amplitude (A_{MAX}) is a function of the ratio at which the helicase falls from a template to the frequency at which it completely unwinds a duplex and is thus a measure of the processivity of unwinding.

RESULTS

Expression and purification of the HCV helicase from genotypes 1a, 1b, and 2a. This project was initiated as an attempt to elucidate the molecular differences between HCV genotypes 1 and 2, the most common genotypes in North America. The HCV helicase was chosen for analysis because it can be relatively easily expressed and purified as a recombinant protein and because the helicase is a popular target for rational HCV drug design. The helicase proteins described here are truncated and lack the first 166 amino acids of the mature HCV NS3 protein. The HCV helicase fragment is used in order to simplify analysis and because the full-length proteins from genotypes 1a and 2a are expressed poorly in *E. coli.* In our experience, both the full-length NS3 and single-chain recombinant NS3-NS4A proteins (16) from genotypes 1a and 2a form mainly insoluble inclusion bodies.

The recombinant HCV helicase proteins were derived from full-length, infectious cDNA clones of HCV genotypes 1a, 1b, and 2a. Recombinant purified helicase from genotype 1a (Hel-1a) contains amino acids 1193 to 1658 of the HCV strain H77 polyprotein (NCBI accession no. AAB67036 [42]). Helicase from genotype 1b (Hel-1b) possesses residues 1193 to 1658 of strain HC-J4 (NCBI accession no. AAC15722 [43]), and helicase from genotype 2a (Hel-2a) contains residues 1197 to 1662 of the polyprotein expressed by HCV strain HC-J6(CH) (NCBI accession no. AAF01178 [41]).

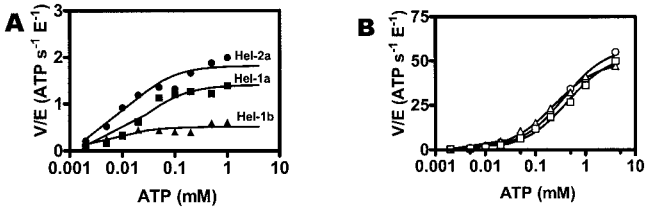

FIG. 1. Steady-state rates of ATP hydrolysis catalyzed by HCV helicases from genotypes 1a, 1b, and 2a. The rate of phosphate release from [γ-^{32}P]ATP was monitored at different concentrations of ATP in the absence (A) or presence (B) of 2 mg of poly(U) RNA/ml. Rates were obtained by using Hel-1a (squares), Hel-1b (triangles), or Hel-2a (circles). The data were fit to equation 1 by nonlinear regression analysis to yield the constants summarized in Table 2.

Each of the three recombinant helicases contains the same C-terminal fusion peptide with a polyhistidine tag. Each was expressed in the same cell line [BL21(DE3)] and purified with the same protocol. No differences were noted regarding their relative affinities for the columns used during purification. However, the helicases were expressed at different levels in *E. coli.* Cells containing plasmids expressing Hel-1b consistently produced more protein than cells expressing either Hel-1a or Hel-2a. Typically, 1-liter cultures yield approximately 8 to 10 mg of Hel-1b, 4 to 5 mg of Hel-2a, and 2 to 3 mg of Hel-1a.

Hydrolysis of ATP by helicases isolated from different genotypes. ATPase assays of the three purified helicases are shown in Fig. 1. Initial rates of [γ-^{32}P]ATP hydrolysis were measured for the three helicases at different concentrations of ATP. Under these conditions, velocity was linear with both time and enzyme concentration. Differences between the enzymes were most apparent in the absence of NAs (Fig. 1A). In the absence of NAs, Hel-1b was significantly less active (lower V/E) than either Hel-1a or Hel-2a. However, in the presence of RNA, all three helicases hydrolyzed ATP at similar rates (Fig. 1B). When the data were fit to the Michaelis-Menten equation (equation 1), it became apparent that the presence of NA, in this case, poly(U) RNA, not only stimulates the hydrolysis of ATP but also dramatically decreases the affinity of the enzymes for ATP (Table 2). The data shown in Fig. 1 and Table 2 are expressed as the rate of hydrolysis per mole of enzyme. The apparent K_m of ATP in the absence of poly(U) RNA for Hel-1a, Hel-1b, and Hel-2a decreased 19-fold, 46-fold, and 30-fold, respectively, when RNA was present. The apparent k_{cat} of ATP hydrolysis by Hel-1a increased 38-fold in the presence of poly(U) RNA. Under the same conditions, the k_{cat} of the Hel-1b-catalyzed reaction increased 98-fold, and in the Hel-2a-catalyzed reaction, k_{cat} increased 32-fold. The greater stimulation of Hel-1b is due entirely to its lower basal ATPase level.

Stimulation of NS3 ATPase by NAs. Because helicase is an NA-activated ATPase, another kinetic constant (K_{NA}) could be defined that describes the concentration of the DNA or RNA that supports half the maximum rate of NTP hydrolysis. To determine K_{NA}, each helicase was titrated with poly(U) at saturating levels of ATP (4 mM, approximately 10 to 20 times the K_m). The resulting data are shown in Fig. 2. As seen with a single concentration of NA (Fig. 1), RNA stimulated ATP hydrolysis by each helicase. The data were fit to equation 2 to yield the K_{NA} values listed in Table 2 and another estimate of stimulated k_{cat}, which was in good agreement with the stimulated k_{cat} determined from experiments in Fig. 1B. The average of the two stimulated k_{cat} values is listed in Table 2. Each helicase bound poly(U) with a similar affinity and, under these optimal conditions, hydrolyzed ATP at similar rates.

TABLE 2. Kinetic constants[a] describing the hydrolysis of the four canonical NTPs by the NS3 helicase derived from genotypes 1a, 1b, and 2a

NTP and kinetic constants	Hel-1a	Hel-1b	Hel-2a
ATP			
Stimulated k_{cat} (s^{-1})	54 ± 4	49 ± 5	58 ± 4
Stimulated K_m (μM)	440 ± 90	230 ± 100	370 ± 90
Basal k_{cat} (s^{-1})	1.4 ± 0.1	0.5 ± 0.1	1.8 ± 0.2
Basal K_m (μM)	23 ± 9	5 ± 2	12 ± 4
PolyU K_{NA} (mM)	1.0 ± 0.2	1.2 ± 0.5	0.77 ± 0.1
GTP			
Stimulated k_{cat} (s^{-1})	33 ± 2	41 ± 11	32 ± 2
Stimulated K_m (μM)	1.4 ± 0.6	0.76 ± 0.1	0.98 ± 0.1
Basal k_{cat} (s^{-1})	2.5 ± 0.5	1.3 ± 0.1	2.0 ± 0.6
Basal K_m (μM)	45 ± 6	33 ± 10	45 ± 10
Poly(U) K_{NA} (mM)	0.49 ± 0.2	1.1 ± 0.4	0.21 ± 0.05
CTP			
Stimulated k_{cat} (s^{-1})	29 ± 5	29 ± 4	36 ± 2
Stimulated K_m (μM)	0.26 ± 0.1	0.16 ± 0.05	0.31 ± 0.06
Basal k_{cat} (s^{-1})	1.4 ± 0.01	1.3 ± 0.5	1.6 ± 0.1
Basal K_m (μM)	19 ± 5	5 ± 2	11 ± 2
Poly(U) K_{NA} (mM)	0.45 ± 0.1	0.84 ± 0.03	0.35 ± 0.06
UTP			
Stimulated k_{cat} (s^{-1})	31 ± 3	35 ± 3	38 ± 3
Stimulated K_m (μM)	0.36 ± 0.1	0.23 ± 0.04	0.49 ± 0.2
Basal k_{cat} (s^{-1})	2.0 ± 0.2	1.2 ± 0.03	1.8 ± 0.4
Basal K_m (μM)	28 ± 5	8 ± 4	17 ± 3
Poly(U) K_{NA} (mM)	0.36 ± 0.05	0.70 ± 0.1	0.24 ± 0.07

[a] Kinetic constants were determined for NS3 helicase isolated from genotype 1a (Hel-1a), genotype 1b (Hel-1b), and genotype 2a (Hel-2a). Each constant was determined from three separate titrations done at different enzyme concentrations. Errors represent the variation seen between separate experiments.

HCV NS3 helicase NTPase substrate specificity. The kinetic constants for each of the canonical cellular NTPs were deter-

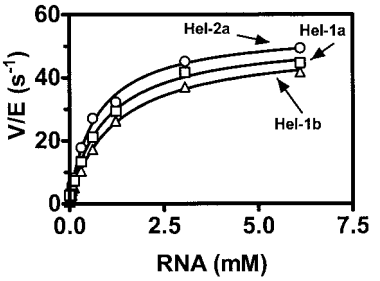

FIG. 2. RNA stimulation of ATP hydrolysis catalyzed by Hel-1a, Hel-1b, or Hel-2a. Steady-state rates of ATP hydrolysis catalyzed by Hel-1a (squares), Hel-1b (triangles), or Hel-2a (circles) were measured in the presence of nine different concentrations of poly(U). The experiments were repeated with three different amounts of enzyme, and average turnover rates (moles of ATP hydrolyzed/moles of enzyme/second) were plotted. The data were fit to equation 2, and the curves were drawn by using the resulting constants (Table 2).

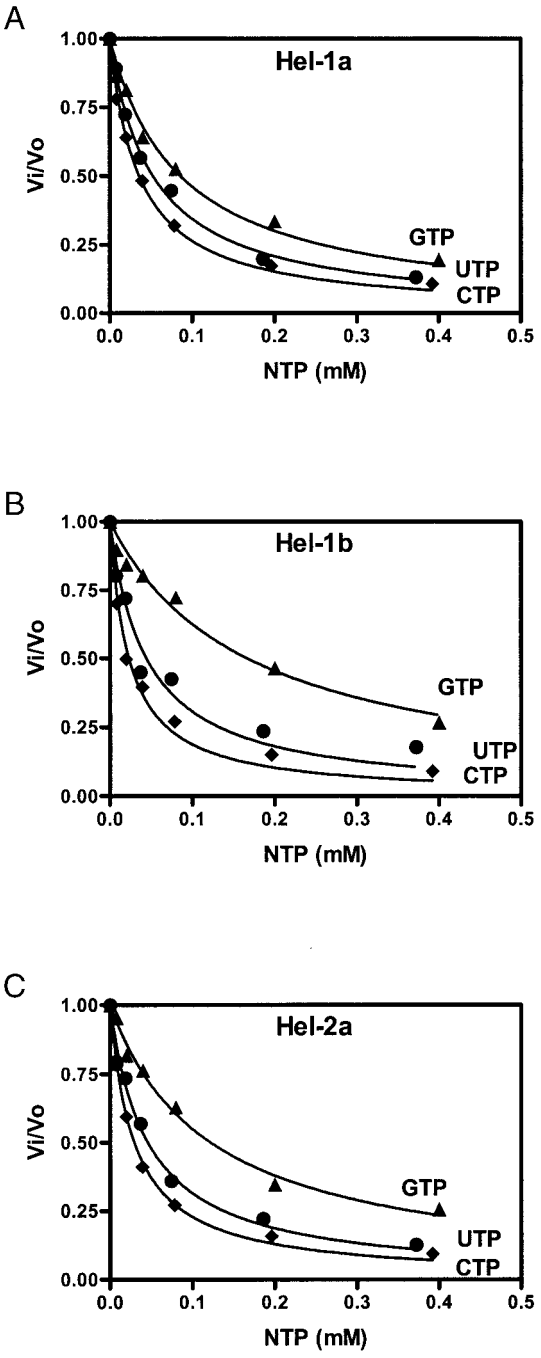

FIG. 3. Inhibition of ATP hydrolysis catalyzed by Hel-1a, -1b, and -2a. Inhibition of reactions containing 50 μM [γ-^{32}P]ATP by GTP (triangles), CTP (diamonds), or UTP (circles) is shown. Reactions were catalyzed by Hel-1a (A), Hel-1b (B), or Hel-2a (C). Data were fit to equation 3 to yield the constants summarized in Table 2.

mined for Hel-1a, Hel-1b, and Hel-2a (Fig. 3; Table 2). To determine the basal k_{cat} [k_{cat} in the absence of NAs] and the K_{NA}, the RNA titrations shown in Fig. 2 were repeated, substituting another NTP for ATP (data not shown). The results are summarized in Table 2. The relative affinities of the helicases for various NTPs were then determined from inhibition experiments (Fig. 3). In such experiments, initial rates for [γ-^{32}P]ATP hydrolysis were measured in the presence and absence of GTP, CTP, or UTP. Data were fit to an equation describing competitive inhibition (equation 3) by using the previously determined K_m values of ATP (Table 2). K_m values for GTP, CTP, and UTP were assumed equivalent to the K_i values determined from equation 3 because the other NTPs were hydrolyzed at rates similar to those for ATP. The results are summarized in Table 2.

All three helicases hydrolyzed the four canonical NTPs at similar rates in the absence of NAs. Under stimulated conditions, all three enzymes hydrolyzed ATP the fastest, although the other NTPs were cleaved 50 to 80% as rapidly. In both the presence and absence of RNA, there were noticeable differences in the affinity of helicase for the various NTPs. Interestingly, under all conditions, GTP bound the enzymes less tightly while the pyrimidine nucleotides bound with an affinity similar to that for ATP (Fig. 3; Table 2). The relative specificities in terms of affinity or catalytic efficiency (k_{cat}/K_m) of the three enzymes were difficult to compare because of the large errors on some kinetic constants, but the only NTP that was hydrolyzed significantly less efficiently was GTP. Thus, the relative catalytic efficiencies were generally ATP $\geq$ CTP $\approx$ UTP $>$ GTP for each enzyme. Similar results were obtained with deoxynucleoside triphosphates (data not shown).

The only apparent difference regarding NTP preference was that Hel-1a is less discriminating between GTP and the other NTPs. As seen in Fig. 3, GTP bound relatively more tightly to Hel-1a than to either Hel-1b or Hel-1a. From the resulting data, shown in Table 2, Hel-1a bound ATP only 1.9-fold more tightly than GTP. In the absence of RNA, Hel-1b bound ATP 6.6-fold more tightly and Hel-2a bound ATP 3.7-fold more tightly than it bound GTP. This difference was not apparent, however, in the presence of stimulating poly(U) RNA.

Helicase template specificity. Unlike related proteins, reports indicate that HCV NS3 NTPase is more stimulated by certain NA sequences (35). The fact that HCV helicase is preferentially stimulated by poly(U) RNA has led to the speculation that the enzyme initiates its action at the polypyrimidine stretch of the 3′ untranslated region of the HCV genome, and some binding data support this hypothesis (2). The effect of various NAs on Hel-1a-, Hel-1b-, and Hel-2a-catalyzed ATP hydrolysis was therefore examined to determine whether this distinctive stimulation profile is a conserved property.

Various NAs were titrated into reactions monitoring ATP hydrolysis by HCV helicase. Such titrations, analogous to those shown in Fig. 2, yielded estimates of k_{cat} and K_{NA} for each template and each helicase (Fig. 4). Template preferences could be due to enhanced binding (K_{NA} effect) or an enhanced turnover rate (k_{cat} effect). ATP hydrolysis by the various helicases was analyzed with RNA homopolymers and DNA oligonucleotides of defined lengths. Because the lengths of the NAs vary, NA concentrations are reported in terms of nucleotide concentration as opposed to the concentration of 3′ ends. The various templates not only bound the helicase with different affinities (Fig. 4B) but also promoted vastly different maximum rates of ATP hydrolysis (Fig. 4A).

The clearly higher affinity (lower K_{NA} [Fig. 4B]) of the enzyme for poly(U) explains its previously reported template preference (35). In addition, as observed by others, poly(G) failed to stimulate the helicase (35). Among RNA homopolymers, the enzyme preferentially bound poly(U) over poly(C) or

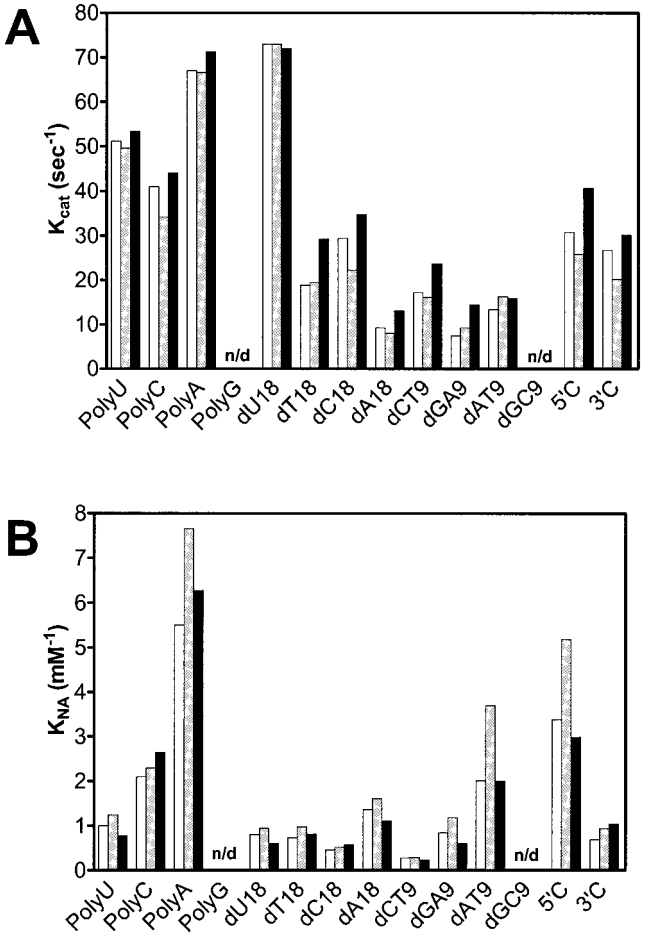

FIG. 4. Template preferences of the various HCV helicases. In experiments analogous to those shown in Fig. 2, the steady-state rate of hydrolysis of ATP by HCV helicase isolated from three genotypes was monitored in the presence of nine different concentrations of various NA templates. Several rates were obtained at NA concentrations above and below each calculated K_{NA}. Data were fit to equation 2 to yield the maximum turnover rate k_{cat} (A) and an apparent affinity, K_{NA}, of the enzyme for each activator (B). In each panel, the bars represent the values obtained with Hel-1a (white), Hel-1b (gray), or Hel-2a (black). Template sequences are listed in Table 1. Kinetic constants were not determined (n/d) for sequences that did not stimulate ATP hydrolysis.

poly(A); however, at saturating NA concentrations, all three templates supported similar k_{cat} values (Fig. 4A). Unlike their ribonucleotide counterparts, however, the homopolymeric DNA templates supported very different maximum rates of ATP hydrolysis. For example, dU18 stimulated ATP hydrolysis more than sevenfold better than dA18 or the polypurine template dGA9 (dG18 could not be synthesized for technical reasons). In general, pyrimidine templates stimulated higher k_{cat} values than purine templates. As seen with the RNA templates, purine-containing DNAs stimulated the enzyme less efficiently than that with pyrimidine templates (compare dA18 to dT18 or dC18; compare dGA9 to dCT9 [Fig. 4B]).

Another explanation for the disparity in NA stimulation could be the secondary structures formed by the NAs. For example, the failure of poly(G) to stimulate hydrolysis might be due to its propensity to form complex structures. To test this hypothesis, DNA oligonucleotides that form hairpin dimers were tested for their ability to stimulate the HCV NS3 ATPase. The first two of these templates, dAT9 and dGC9, can form either duplex DNA (because they are self complementary) or stable 9-bp hairpins. As suspected, dGC9, which forms a stable duplex, did not stimulate hydrolysis. However, at saturating levels, dAT9 stimulated hydrolysis similar to that of the polypurine template dGA9 (Fig. 4A). AT9 formed a less stable duplex than GC9 because fewer hydrogen bonds were formed in A · T base pairs. There is a clear two- to fourfold difference in the affinity of the helicase for dAT9 compared with that of templates less likely to form stable base pairs (Fig. 4B). The ability of dAT9 to stimulate ATP hydrolysis suggests that some of this template is present in a single-stranded form.

HCV helicase requires a 3′ single-stranded region in order to initiate strand separation (36), and the 3′-to-5′ polarity of helicase translocation has recently been confirmed (27). Templates 5′C and 3′C were used to assess the effect of the polarity of single-stranded regions on ATPase stimulation. Template 3′C is identical to dGC9 except for a 3′ poly(C) tail. Likewise, template 5′C is identical to dGC9 except for a 5′ poly(C) tail. Unlike dGC9, both 5′C and 3′C stimulate the NS3 ATPase, indicating that the helicase can bind to both 3′ and 5′ single-stranded regions, as has been previously reported (36). Interestingly, the enzymes clearly differentiated between substrates with 5′ and 3′ ssDNA tails (Fig. 4B). In fact, template 3′C stimulated each enzyme three- to fivefold more efficiently than template 5′C, suggesting that the location of the duplex region plays a role in stabilizing the template in its binding site.

Binding assays. The above data strongly suggest that HCV helicase preferentially binds certain DNA sequences. However, K_{NA} is a kinetic constant and may not reflect a true dissociation constant if HCV helicase and NA are not in a state of rapid equilibrium. In addition, ATP hydrolysis and subsequent protein translocation likely affect the apparent affinity for certain templates. Two methods were utilized to examine more directly the interaction of NAs with HCV helicase: gel shift assays and fluorimetric binding equilibrium titrations. These studies focused on two oligonucleotides, one containing only pyrimidines (dCT9) and a second that contained only purines (dGA9). Oligonucleotide dCT9 activated all three helicases to a higher k_{cat} than dGA9 (Fig. 4A) and did so with a lower K_{NA} (Fig. 4B).

In gel shift assays (Fig. 5), increasing amounts of helicase (up to 1 mM) were incubated with the same amount of a radiolabeled DNA oligonucleotide (200 nM). After 10 min at room temperature, the complexes were separated on native polyacrylamide gels and the percentage of bound DNA (shifted) was determined by image analysis. In such assays, it was immediately apparent that more protein was required to shift 50% of dGA9 than was necessary to shift 50% of dCT9 (Fig. 5B). All three helicases retained this sequence specificity, and all had about the same relative affinity for the DNA (Fig. 5B).

The gel shift studies likely underestimate the protein-DNA binding because equilibrium is perturbed during electrophoresis. Therefore, another method was used to determine DNA binding by the helicase under equilibrium conditions. Because HCV helicase has an exposed tryptophan near the ssDNA-binding site (18), DNA binding could be measured by moni-

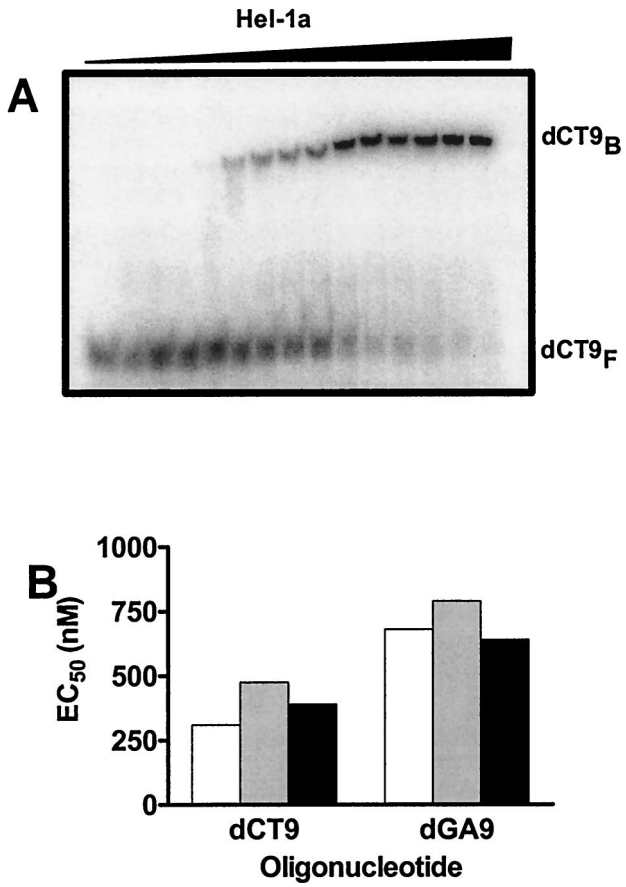

FIG. 5. Gel shift analysis of DNA binding by the HCV helicase. (A) In 10-μl reactions, various amounts of Hel-1a were incubated with 200 nM radiolabeled CT9. After 10 min at room temperature, bound ($dCT9_B$) and free ($dCT9_F$) DNA were separated by native polyacrylamide gel electrophoresis. The reactions that were analyzed in lanes 1 through 15 in panels A and B contained, respectively, 0, 114, 133, 152, 175, 190, 228, 226, 304, 357, 408, 456, 532, 608, and 760 nM of Hel-1a. (B) The experiment was repeated with Hel-1b and also with Hel-2a with radiolabeled dCT9 and dGA9 to determine the concentration of protein required to shift 50% of the radiolabeled oligonucleotide (EC_{50}).

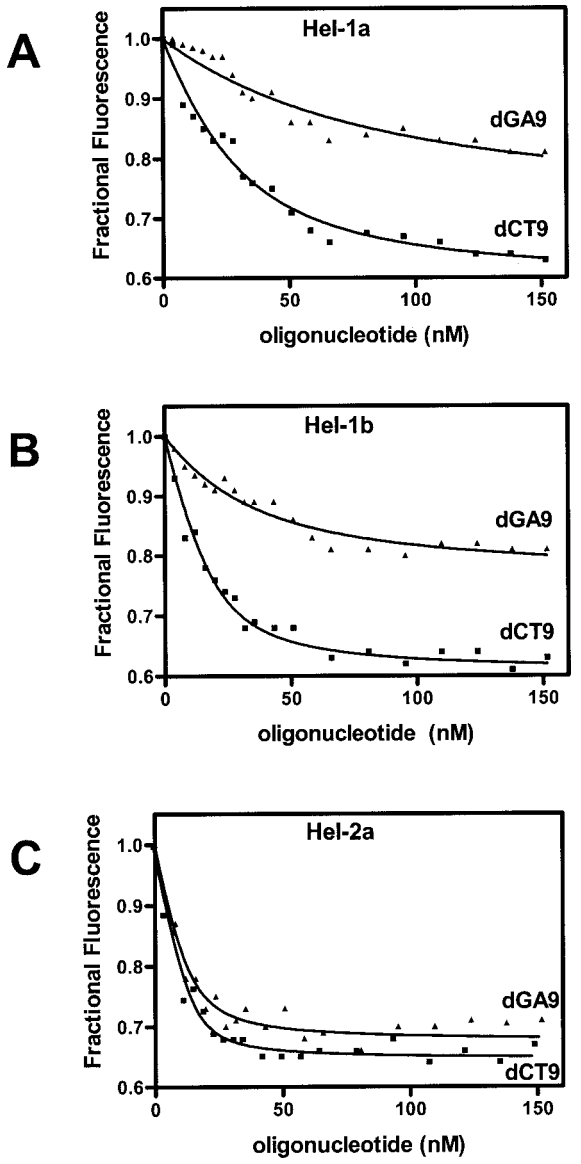

FIG. 6. Quenching of the intrinsic protein fluorescence of HCV helicase by NAs. Oligonucleotides dCT9 (■) or dGA9 (●) (0 to 151.6 nM) were added to 12 nM Hel-1a (A), 18 nM Hel-1b (B), or 22 nM Hel-2a (C), and intrinsic protein fluorescence was measured (λ_{ex} = 280, λ_{em} = 340). Fractional fluorescence remaining at each NA concentration was determined, and data were fit to equation 5. Resulting changes in intrinsic protein fluorescence and the apparent dissociation constants are summarized in Table 3.

toring intrinsic protein fluorescence. As the template binds, the protein fluorescence was quenched, as shown in Fig. 6. As shown by others (21, 33), nonlinear regression analysis of such data yields a maximum fluorescence change (ΔF_{MAX}) and an apparent dissociation constant (K_D).

Clear differences between Hel-2a and the helicase isolated from genotype 1 strains were noted in these titrations monitoring protein fluorescence (Fig. 6; Table 3). First, Hel-2a bound the oligonucleotides the most tightly. Oligonucleotide dCT9 bound Hel-2a 10 times more tightly than Hel-1a and 3 times more tightly than Hel-1b. Similarly, dGA9 bound Hel-2a 25-fold tighter than Hel-1a and 10-fold tighter than Hel-1b. With both Hel-1a (Fig. 6A) and Hel-1b (Fig. 6B), templates composed of pyrimidines quenched protein fluorescence more effectively than those composed of purines quenched fluorescence. However, when the same experiment was repeated with Hel-2a (Fig. 6C), both oligonucleotides quenched fluorescence to a similar extent. The data in Table 3 clearly shows that K_D is sequence dependent. Previous studies (21, 33) have only shown that K_D is length dependent (short templates bind more weakly). The absolute values for the binding constants for dCT9 to HCV helicase (Table 3) were in the same range as those reported for other pyrimidine-containing templates (21, 33, 34).

Hel-2a unwinds DNA more rapidly than Hel-1a and Hel-1b. It is difficult to measure helicase unwinding under steady-state conditions because when substrate (duplex NA) is in excess over enzyme, it is likely that the ssDNA products will reanneal before unwinding can be observed. For this reason, most he-

TABLE 3. Oligonucleotide binding by HCV helicase[a]

Helicase	dCT9		dGA9	
	K_D (nM)	ΔF_{MAX}	K_D (nM)	ΔF_{MAX}
Hel-1a	16 ± 3	0.41	71 ± 25	0.30
Hel-1b	5 ± 1.5	0.39	36 ± 6	0.23
Hel-2a	1.6 ± 0.3	0.32	2.8 ± 0.5	0.32
T450I	13 ± 4	0.34	9.1 ± 4	0.25

[a] The maximum change in intrinsic protein fluorescence (ΔF_{MAX}) and apparent dissociation constant (K_D) were determined by fitting the data shown in Fig. 6 to equation 5.

licase assays are done with a very low concentration of substrate and excess helicase. Under such conditions, all three helicases examined here unwound duplex DNA, RNA, and DNA/RNA heteroduplexes, but no differences were noted among the helicases (data not shown). The helicase assays were therefore repeated in the presence of excess NA to act as an enzyme trap (Fig. 7A). When a trap is included in helicase assays, it prevents free enzymes from binding partially unwound substrate after an initially bound enzyme dissociates from the template. Thus, both unwinding rate and processivity can be assessed in a single-turnover assay. In single-turnover assays, clear differences were noted in the abilities of the helicases to unwind duplex NAs (Fig. 7A). The NA substrates used for the assay shown in Fig. 7 contained a template strand with a 3′ overhang annealed to a γ-^{32}P-labeled release strand (for sequences, see Table 1). NA and HCV helicase were preincubated, and the reactions were initiated by the addition of ATP and excess trap NA, which was made of the same NA sequence as the release strand. Reactions were terminated, separated on a 12% native polyacryamide gel, and analyzed with a phosphorimager. Figure 7A shows that all three helicases purified here shared a decreased ability to processively unwind RNA. The low processivity of HCV helicase on RNA compared to that on DNA was recently reported in a study using the full-length NS3 protein from the H-strain of HCV genotype 1a (29). The nature of the template strand appears to primarily determine enzyme processivity. A heteroduplex with a 3′ DNA tail (RNA/3′ DNA) was unwound almost as well as duplex DNA, whereas a heteroduplex with an ssRNA tail (DNA/3′ RNA) was unwound poorly.

It is also apparent from the data in Fig. 7A that Hel-2a appears to unwind NA faster than the other two enzymes. To investigate this effect in more detail, HCV helicase assays were performed under single-turnover conditions to measure k_{obs} and A_{MAX}. The amplitude is a function of the ratio at which the helicase falls from a template to the frequency at which it completely unwinds a duplex and is thus a measure of the processivity of unwinding. The assays were performed with DNA because RNA was not processively unwound by the enzymes (Fig. 7A).

To determine the above constants describing unwinding kinetics, unwound DNA at various times was fit to equation 6. The results (Fig. 7B) indicate that the three helicases functioned with somewhat different rates and processivities. Hel-1a and Hel-1b unwound DNA more slowly, whereas Hel-2a unwound more rapidly, with a higher apparent processivity. The differences were minor, however, and rates varied by less than twofold.

Genetic differences. Alignments of the three helicase proteins (Fig. 8A) revealed that Hel-1a and Hel-1b share 92% identical amino acids. Amino acid residues were numbered from the start of the full-length NS3 protein containing the HCV serine protease. Hel-1a and Hel-2a were 85% identical, and likewise, Hel-1b and Hel-2a had 85% of their residues in common.

As seen in Fig. 8A, there was significant variation near the six conserved helicase motifs. Motif I (GSGKS) was a Walker-type (P-loop) nucleotide-binding site and was absolutely conserved among Hel-1a, Hel-1b, and Hel-2a. The second motif contained the DECH (DEAD-box-like, or DExD/H-box) signature sequence. Although the DECH sequence was conserved, the residues immediately following this sequence varied. The sequence around motif II in Hel-1a was DECHSTDA, the sequence around motif II in Hel-1b was DECHSTDS, and the sequence for Hel-2a was DECHAVDS. Near motif III (VLATAT), residue 318 differed between genotypes 1 and 2. Residue 318 was a Val in Hel-1a and Hel-1b and a Thr in Hel-2a. No variation was seen in the conserved motifs IV

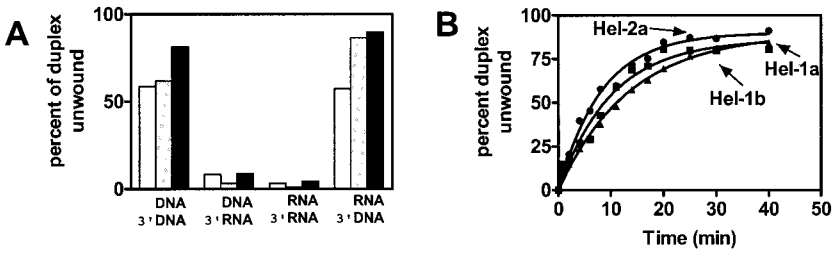

FIG. 7. Helicase activity of Hel-1a, Hel-1b, and Hel-2a. (A) Helicase action on duplex DNA, RNA, and DNA/RNA heteroduplexes in the presence of an NA trap. One heteroduplex (DNA/3′ RNA) contained a template strand with a single-stranded tail made of RNA, and the other (RNA/3′ DNA) had a DNA template strand and an RNA release stand. Substrate (2 nM) was incubated with 280 nM Hel-1a (white), Hel-1b (gray), or Hel-2a (black) for 30 min and initiated with ATP (5 mM) and trap DNA (3 μM). Reactions were terminated after 10 min at room temperature, and the percentage of DNA unwound was determined by analyzing the products separated on 12% native polyacrylamide gels. (B) Rates of helicase action. DNA/3′ DNA substrate (1 nM) was incubated with 280 nM Hel-1a (■), Hel-1b (▲), or Hel-2a (●) for 10 min at room temperature before initiating the reaction with ATP (5 mM) and trap DNA (3 μM). Reactions were terminated at various times, and the percentage of DNA unwound was determined. Data were fit to equation 6 to yield the following: for Hel-1a, an A_{MAX} of 86% and k_{obs} of 0.099 min^{-1}; for Hel-1b, an A_{MAX} of 88% and k_{obs} of 0.073 min^{-1}; and for Hel-2a, an A_{MAX} of 91% and k_{obs} of 0.12 min^{-1}.

A

```
                                                          [ I  ]
Hel-1a 167 VDFI PVENLGTTMR SPVFTDNSSP PAVPQSFQVA HLHAPTGSGK STKVPA 216
Hel-1b 167 .... ...SME.... ........T. .....T.... .......... ...... 216
Hel-2a 167 I... ...T.DIVT. ..T.S...T. .....TY..G Y......... .....V 216

Hel-1a 217 AYAA QGYKVLVLNP SVAATLGFGA YMSKAHGVDP NIRTGVRTIT TGSPIT 266
Hel-1b 217 .... .......... .......... .......I.. .......... ..GS.. 266
Hel-2a 217 .... .......... .......... .L.....IN. ........V. ..A... 266

                                  [ II ]
Hel-1a 267 YSTY GKFLADGGCS GGAYDIIICD ECHSTDATSI LGIGTVLDQA ETAGAR 316
Hel-1b 267 .... .......... .......... ......S.T. .......... ...... 316
Hel-2a 267 .... .........A .......... ...AV.S.T. .......... ....V. 316

             [ III ]                                              [
Hel-1a 317 LVVL ATATPPGSVT VSHPNIEEVA LSTTGEIPFY GKAIPLEVIK GGRHLI 366
Hel-1b 317 .... .......... .P......IG ..NN...... .....I.A.. ...... 366
Hel-2a 317 .T.. .......... TP........ .GQE...... .R....SY.. ...... 366

            IV    ]                                        [   V
Hel-1a 367 FCHS KKKCDELAAK LVALGINAVA YYRGLDVSVI PTSGDVVVVS TDALMT 416
Hel-1b 367 .... .......... .TG..L.... .......... .PI......A ...... 416
Hel-2a 367 .... .........A .RGM.L.S.. .......... ..Q......A ...... 416

          ]                                                  [   VI
Hel-1a 417 GFTG DFDSVIDCNT CVTQTVDFSL DPTFTIETTT LPQDAVSRTQ RRGRTG 466
Hel-1b 417 .... .......... .......... .......... V.......S. ...... 466
Hel-2a 417 .Y.. .........V A...V..... ......T.QI V.......S. ...... 466

            ]
Hel-1a 467 RGKP GIYRFVAPGE RPSGMFDSSV LCECYDAGCA WYELTPAETT VRLRAY 516
Hel-1b 467 ..RS ......T... .......... .......... .........S ...... 516
Hel-2a 467 ..RL ....Y.ST.. .A......V. ........A. ......S... ...... 516

Hel-1a 517 MNTP GLPVCQDHLE FWEGVFTGLT HIDAHFLSQT KQSGENFPYL VAYQAT 566
Hel-1b 517 L... .......... ...S...... .......... ..A.D..... ...... 566
Hel-2a 517 F... .......... ...A...... .......... .......A.. T..... 566

Hel-1a 567 VCAR AQAPPPSWDQ MWKCLIRLKP TLHGPTPLLY RLGAVQNEVT LTHPIT 616
Hel-1b 567 .... .......... .......... .......... .........I ...... 616
Hel-2a 567 .... .K.......V .....T.... ..V....... ...S.T.... ....V. 616

Hel-1a 617 KYIM TCMSADLEVV T 631
Hel-1b 617 .... A......... . 631
Hel-2a 617 ...A ...Q.....M . 631
```

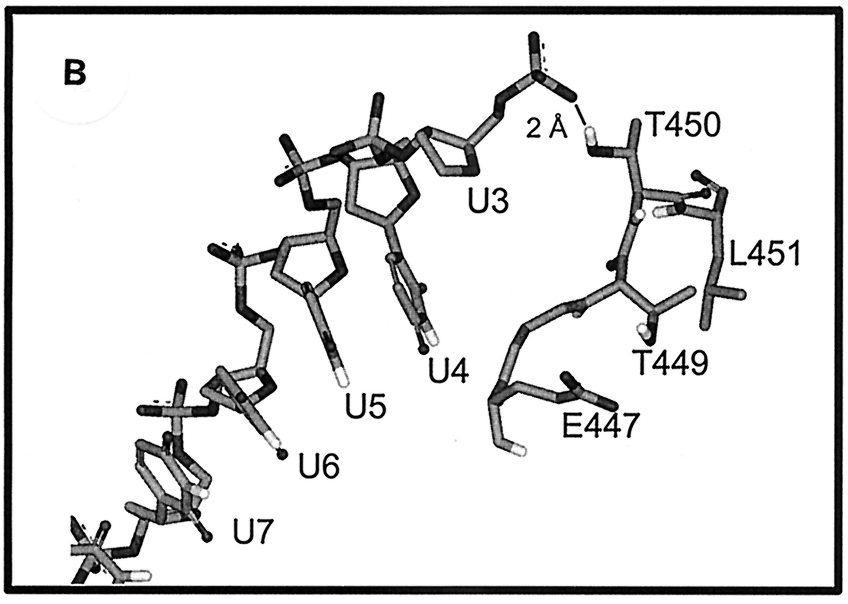

FIG. 8. Genetic difference among the helicases from HCV genotypes 1a, 1b, and 2a. (A) Alignment of Hel-1a (NCBI accession no. AAB67036), Hel-1b (NCBI accession no. AAC15722), and Hel-2a (NCBI accession no. AAF01178) (41). Residues in Hel-1b and Hel-2a that were identical to Hel-1a are noted as dots. Conserved motifs (13) are noted within brackets. (B) Variants amino near the NA binding site of the HCV helicase. The side chain hydroxyl of residue T450 was free to rotate to within 2 Å of the phosphate backbone, where it could donate a hydrogen bond. Coordinates are from Protein Data Bank accession code 1A1V.

(LIFCHSKKK), V (TDALMTG), or VI (QRRGRTGR). However, there were differences among genotypes 1a, 1b, and 2a in the 2 amino acids flanking motif V. At position 410, the N terminus of motif V near the bound DNA, genotype 1a had a serine whereas genotypes 1b and 2a each had an alanine. At position 418, genotypes 1a and 1b had a phenylalanine but genotype 2a had a tyrosine.

Variant residues that could play a role in RNA binding are likely located in the RNA-binding site of HCV helicase (Fig. 8B). Several residues vary in the region located near the 5′ end of the DNA in a co-crystal structure with HCV helicase (18). In the structural models of NS3 with bound DNA (18), one of these residues, T450, was positioned to interact with the phosphate backbone. However, this residue was not conserved in all genotypes (Fig. 8A), and in Hel-2a, NS3 residue 450 was an isoleucine. The helicase from genotype 2a (Hel-2a) bound DNA more tightly (Fig. 6) and unwound DNA more rapidly (Fig. 7) than Hel-1a or Hel-1b.

NS3 residue 450 is critical for NA binding and unwinding. To determine if residue 450 plays a role in imparting distinctive properties in Hel-2a, residue T450 of Hel-1a was changed by site-directed mutagenesis to an isoleucine. The T450I mutant

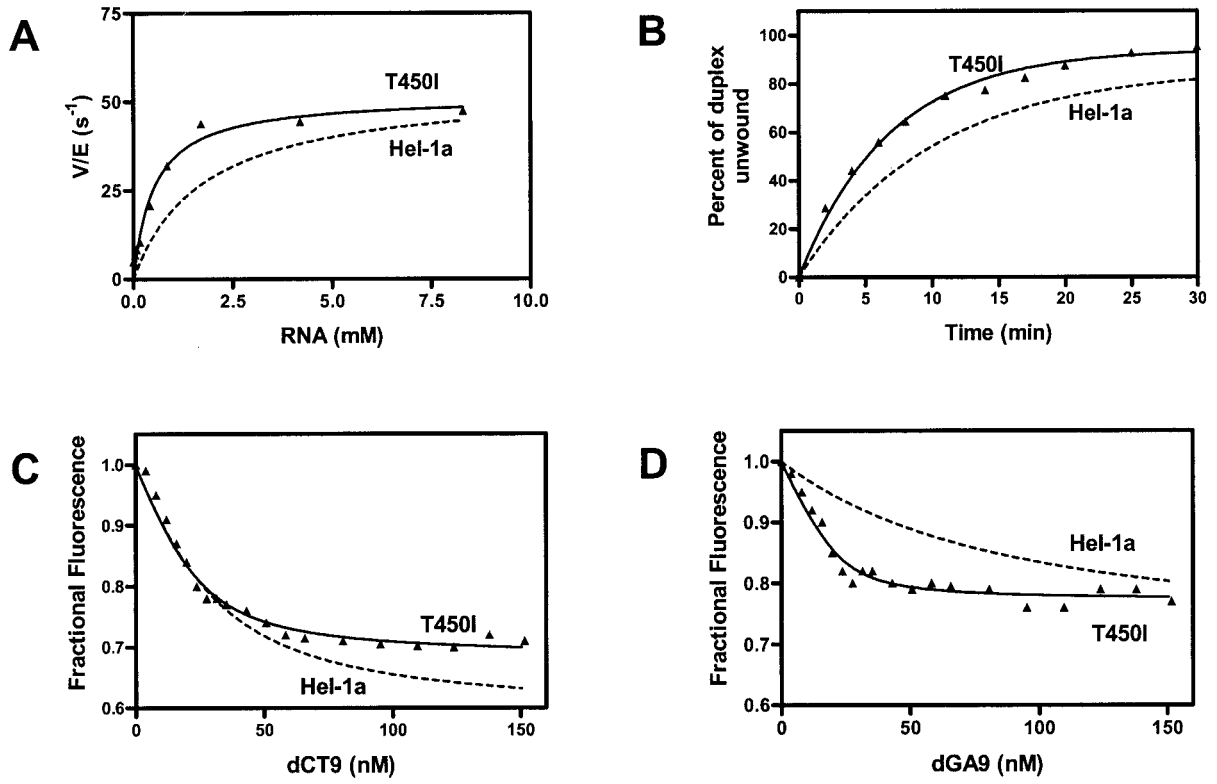

FIG. 9. Comparison of Hel-1a and Hel-1a with a T450I substitution. (A) Steady-state rates of ATP hydrolysis catalyzed at different concentrations of poly(U) RNA are given. Data were fit to equation 2 to yield a k_{cat} of 54 and a K_{NA} of 0.5 mM. (B) Unwinding of duplex DNA by T450I in a single-turnover assay as described in Fig. 7 are shown. Data were fit to equation 6 to yield an A_{max} of 86% and k_{obs} of 0.099 min^{-1} for Hel-1a and an A_{max} of 94% and k_{obs} of 0.15 min^{-1} for T450I. (C and D) Quenching of intrinsic T450I fluorescence was monitored when the protein was titrated with dCT9 (C) or dGA9 (D). Total protein in the titrations was 12 nM, the data were fit to equation 5, and the resulting K_D and ΔF_{MAX} values are listed in Table 3. In each panel, data obtained with Hel-1a, the parent of T450I, are shown as a dotted line.

and the wild-type Hel-1a were both stimulated by RNA (Fig. 9A), but T450I had a K_{NA} about twofold lower than that of Hel-1a. The two proteins also had similar NTP and NA specificities (data not shown). However, like Hel-2a, T450I unwound DNA more rapidly than Hel-1a, with a higher apparent processivity (Fig. 9B). The T450I mutation also dramatically influenced the binding properties of the Hel-1a protein. Like Hel-2a, T450I did not discriminate between dCT9 and dGA9 as well as Hel-1a or Hel-1b (Table 3). In fact, dGA9 bound T450I slightly more tightly than dCT9. This new behavior is due to the fact that T450I bound dGA eightfold more tightly than the wild-type Hel-1a (Fig. 9D), but the mutation did not significantly alter the affinity for dCT9 (Fig. 9C). These data clearly show that T450 plays a significant role in DNA binding and unwinding and that mutation of this residue to isoleucine in Hel-2a could account for some of the distinctive properties of Hel-2a.

DISCUSSION

Three main differences were noted among the HCV helicases isolated from the three distinct HCV genotypes. First, Hel-1b hydrolyzes NTPs more slowly. Second, Hel-1a poorly discriminates among the canonical NTPs. Third, Hel-2a unwinds DNA more rapidly and binds DNA more tightly. Variations near the ATP-binding motifs (Fig. 8) might explain differences in ATPase function, but this hypothesis was not directly tested. However, we have shown by site-directed mutagenesis that variation in the NA-binding cleft likely explains differences in DNA binding and unwinding (Fig. 9). Although these differences are minor in kinetic terms, they could play important roles in the viral life cycle, especially if helicase action limits the rate of viral replication.

One noteworthy conserved property is the enzyme's NA stimulation profile (Fig. 4). When Suzich et al. (35) first isolated the HCV helicase, they noted that the NS3 ATPase was preferentially stimulated by certain NA sequences. This unique polynucleotide stimulation profile distinguishes the HCV enzyme from related cellular proteins (6) and even helicases isolated from the same family of viruses (35). Since then, several other studies have illustrated that HCV helicase binds some sequences, particularly those containing uracil, more tightly (2, 15, 17, 30), and that NS3-catalyzed ATP hydrolysis is preferentially stimulated by certain NAs (26, 33). This template preference is an intrinsic and conserved property of the enzyme (Fig. 4). All three helicases were stimulated similarly by different NA sequences and bound certain sequences composed of pyrimidines more tightly. Some K_{NA} differences (Fig. 4B) might be accounted for because different templates have different propensities to form secondary structures. In other words, the absolute concentration of ssDNA varies for each template.

As shown by the equilibrium binding assays (Fig. 6), some of this NA preference stems from the tighter binding of the helicase to certain sequences. However, NA-binding properties are not conserved between genotypes 1 and 2. For example, Hel-2a binds DNA more tightly than Hel-1a or Hel-1b. In addition, enzymes that do not effectively discriminate between dCT9 and dGA9, such as Hel-2a and T450I, are still stimulated by pyrimidine templates more efficiently than by the purine-containing templates. Tighter binding also does not explain the different maximum hydrolysis rates of ATP supported by different templates (Fig. 4A). At saturating concentrations, not all templates support the same turnover rate of ATP. Such template preferences are quite remarkable, especially in light of the crystal structure of the HCV helicase bound to DNA in which no direct interactions between helicase side chains and nucleotide bases were noted (18). Exactly how and why certain NAs more efficiently stimulate the HCV NS3 ATPase/helicase have not yet been fully explained.

Another property that varies among the helicases is their intrinsic rate of ATP hydrolysis. Hel-1b hydrolyzes ATP slower than the other two helicases. How could a lower basal level of ATPase be linked to the pathogenicity of genotype 1b and its poor response to therapy? The answer may lie in the fact that, in the absence of NAs, HCV helicase still hydrolyzes ATP at a rapid rate (k_{cat} = 0.5 to 3 s^{-1}). Such an activity squanders the precursors necessary for viral replication, especially because HCV helicase does not significantly differentiate between ATP, CTP, and UTP; only GTP interacts with the enzyme with a lower affinity (Table 2). Strains that have evolved to minimize this wasteful activity could replicate more quickly. Alternatively, as pointed out by Aoubala et al. (1), unnecessary NS3-catalyzed cellular ATP hydrolysis could lead to a buildup of AMP, leading to an induction of metabolic stress responses, which could lead to global changes in gene expression and/or the destruction of host cells.

The absolute rate of NTP hydrolysis is not the only variant property of the helicase that could influence the virus life cycle. Slight changes in substrate specificity could also have profound implications. Helicases with relaxed NTP specificity, like Hel-1a, might more rapidly degrade antiviral agents that exert their effects as NTPs. For example, a theory that ribavirin acts as a lethal mutagen to eliminate HCV has been proposed recently (5). To act as a mutagen, ribavirin must first be converted to an NTP and incorporated into viral RNA by the NS5B RNA-dependent RNA polymerase. RTP has been shown to inhibit HCV helicase (3), and in this process, RTP would likely be degraded to ribavirin diphosphate, which is not a substrate for NS5B polymerase. Thus, the indiscriminate nature of the NS3 ATPase could help the virus evade a wide variety of antiviral drugs.

The final difference noted between genotype 1 and 2 helicases was in the rate of DNA unwinding. Hel-2a unwound DNA faster than the other two enzymes. The more efficient unwinding by Hel-2a could be because Hel-2a binds DNA more tightly, which might enhance the processivity of the enzyme. More rapid helicase action might help explain why genotype 2a is more sensitive to therapy if ribavirin indeed functions as a lethal mutagen (5). More rapid RNA unwinding would allow the virus to replicate faster, and faster replication could lead to more incorporation of ribavirin into the viral genome, more mutations, and error catastrophe.

Whereas some of the differences noted in this study, which are minor in kinetic terms, could result simply from subtle unforeseen variations in the enzyme preparations, the distinguishing characteristics of Hel-2a clearly result from genetic variations. We have used site-directed mutagenesis to demonstrate this point. Hel-1a bearing the single point mutation T450I has many of the same characteristics as Hel-2a (Fig. 9). The finding that this nonconserved residue is important for helicase function identifies a new region that is critical for the helicase action outside the motifs conserved among related helicases.

The biological relevance of the genotypic differences in NS3 has not been addressed in this study, but several intriguing ideas can be gleaned from the resultant data. For example, we have suggested that the enhanced unwinding by Hel-2a could be the basis for the non-genotype 1 strains' better response to antiviral therapy. Although such ideas are highly speculative, they could be feasibly tested by measuring mutation rates in HCV replicon systems (14). Current replicons could be modified to contain Hel-2a or simply the T450I substitution. Viral replication rate and fidelity could then be measured in the presence and absence of ribavirin or other antiviral compounds.

ACKNOWLEDGMENTS

This work was supported by the AASLD Liver Scholar Award from the American Liver Foundation and the New York Medical College Castle-Krob Research Endowment.

We thank Fred Jaffe and Ruth Gallagher for valuable technical assistance.

REFERENCES

1. **Aoubala, M., J. Holt, R. A. Clegg, D. J. Rowlands, and M. Harris.** 2001. The inhibition of cAMP-dependent protein kinase by full-length hepatitis C virus NS3/4A complex is due to ATP hydrolysis. J. Gen. Virol. **82:**1637–1646.
2. **Banerjee, R., and A. Dasgupta.** 2001. Specific interaction of hepatitis C virus protease/helicase NS3 with the 3′-terminal sequences of viral positive- and negative-strand RNA. J. Virol. **75:**1708–1721.
3. **Borowski, P., M. Lang, A. Niebuhr, A. Haag, H. Schmitz, J. S. zur Wiesch, J. Choe, M. A. Siwecka, and T. Kulikowski.** 2001. Inhibition of the helicase activity of HCV NTPase/helicase by 1-β-D-ribofuranosyl-1,2,4-triazole-3-carboxamide-5′-triphosphate (ribavirin-TP). Acta Biochim. Pol. **48:**739–744.
4. **Cho, H. S., N. C. Ha, L. W. Kang, K. M. Chung, S. H. Back, S. K. Jang, and B. H. Oh.** 1998. Crystal structure of RNA helicase from genotype 1b hepatitis C virus. A feasible mechanism of unwinding duplex RNA. J. Biol. Chem. **273:**15045–15052.
5. **Crotty, S., C. Cameron, and R. Andino.** 2002. Ribavirin's antiviral mechanism of action: lethal mutagenesis? J. Mol. Med. **80:**86–95.
6. **Du, M. X., R. B. Johnson, X. L. Sun, K. A. Staschke, J. Colacino, and Q. M. Wang.** 2002. Comparative characterization of two DEAD-box RNA helicases in superfamily II: human translation-initiation factor 4A and hepatitis C virus non-structural protein 3 (NS3) helicase. Biochem. J. **363:**147–155.
7. **Enomoto, N., I. Sakuma, Y. Asahina, M. Kurosaki, T. Murakami, C. Yamamoto, Y. Ogura, N. Izumi, F. Marumo, and C. Sato.** 1996. Mutations in the nonstructural protein 5A gene and response to interferon in patients with chronic hepatitis C virus 1b infection. N. Engl. J. Med. **334:**77–81.
8. **Erickson, A. L., Y. Kimura, S. Igarashi, J. Eichelberger, M. Houghton, J. Sidney, D. McKinney, A. Sette, A. L. Hughes, and C. M. Walker.** 2001. The outcome of hepatitis C virus infection is predicted by escape mutations in epitopes targeted by cytotoxic T lymphocytes. Immunity **15:**883–895.
9. **Farci, P., and R. H. Purcell.** 2000. Clinical significance of hepatitis C virus genotypes and quasispecies. Semin. Liver Dis. **20:**103–126.
10. **Farci, P., A. Shimoda, A. Coiana, G. Diaz, G. Peddis, J. C. Melpolder, A. Strazzera, D. Y. Chien, S. J. Munoz, A. Balestrieri, R. H. Purcell, and H. J. Alter.** 2000. The outcome of acute hepatitis C predicted by the evolution of the viral quasispecies. Science **288:**339–344.
11. **Farci, P., R. Strazzera, H. J. Alter, S. Farci, D. Degioannis, A. Coiana, G. Peddis, F. Usai, G. Serra, L. Chessa, G. Diaz, A. Balestrieri, and R. H.**

Purcell. 2002. Early changes in hepatitis C viral quasispecies during interferon therapy predict the therapeutic outcome. Proc. Natl. Acad. Sci. USA **99:**3081–3086.
12. **Frick, D. N., D. J. Weber, J. R. Gillespie, M. J. Bessman, and A. S. Mildvan.** 1994. Dual divalent cation requirement of the MutT dGTPase. Kinetic and magnetic resonance studies of the metal and substrate complexes. J. Biol. Chem. **269:**1794–1803.
13. **Gorbalenya, A. E., E. V. Koonin, A. P. Donchenko, and V. M. Blinov.** 1989. Two related superfamilies of putative helicases involved in replication, recombination, repair and expression of DNA and RNA genomes. Nucleic Acids Res. **17:**4713–4730.
14. **Grakoui, A., H. L. Hanson, and C. M. Rice.** 2001. Bad time for Bonzo? Experimental models of hepatitis C virus infection, replication, and pathogenesis. Hepatology **33:**489–495.
15. **Gwack, Y., D. W. Kim, J. H. Han, and J. Choe.** 1996. Characterization of RNA binding activity and RNA helicase activity of the hepatitis C virus NS3 protein. Biochem. Biophys. Res. Commun. **225:**654–659.
16. **Howe, A. Y., R. Chase, S. S. Taremi, C. Risano, B. Beyer, B. Malcolm, and J. Y. Lau.** 1999. A novel recombinant single-chain hepatitis C virus NS3-NS4A protein with improved helicase activity. Protein Sci. **8:**1332–1341.
17. **Kanai, A., K. Tanabe, and M. Kohara.** 1995. Poly(U) binding activity of hepatitis C virus NS3 protein, a putative RNA helicase. FEBS Lett. **376:**221–224.
18. **Kim, J. L., K. A. Morgenstern, J. P. Griffith, M. D. Dwyer, J. A. Thomson, M. A. Murcko, C. Lin, and P. R. Caron.** 1998. Hepatitis C virus NS3 RNA helicase domain with a bound oligonucleotide: the crystal structure provides insights into the mode of unwinding. Structure **6:**89–100.
19. **Krieger, N., V. Lohmann, and R. Bartenschlager.** 2001. Enhancement of hepatitis C virus RNA replication by cell culture-adaptive mutations. J. Virol. **75:**4614–4624.
20. **Levin, M. K., and S. S. Patel.** 1999. The helicase from hepatitis C virus is active as an oligomer. J. Biol. Chem. **274:**31839–31846.
21. **Levin, M. K., and S. S. Patel.** 2002. Helicase from hepatitis C virus, energetics of DNA binding. J. Biol. Chem. **277:**29377–29385.
22. **Lin, C., and J. L. Kim.** 1999. Structure-based mutagenesis study of hepatitis C virus NS3 helicase. J. Virol. **73:**8798–8807.
23. **Locatelli, G. A., G. Gosselin, S. Spadari, and G. Maga.** 2001. Hepatitis C virus NS3 NTPase/helicase: different stereoselectivity in nucleoside triphosphate utilisation suggests that NTPase and helicase activities are coupled by a nucleotide-dependent rate limiting step. J. Mol. Biol. **313:**683–694.
24. **Lohmann, V., F. Korner, A. Dobierzewska, and R. Bartenschlager.** 2001. Mutations in hepatitis C virus RNAs conferring cell culture adaptation. J. Virol. **75:**1437–1449.
25. **McHutchison, J. G., S. C. Gordon, E. R. Schiff, M. L. Shiffman, W. M. Lee, V. K. Rustgi, Z. D. Goodman, M. H. Ling, S. Cort, J. K. Albrecht, et al.** 1998. Interferon alfa-2b alone or in combination with ribavirin as initial treatment for chronic hepatitis C. N. Engl. J. Med. **339:**1485–1492.
26. **Morgenstern, K. A., J. A. Landro, K. Hsiao, C. Lin, Y. Gu, M. S. Su, and J. A. Thomson.** 1997. Polynucleotide modulation of the protease, nucleoside triphosphatase, and helicase activities of a hepatitis C virus NS3-NS4A complex isolated from transfected COS cells. J. Virol. **71:**3767–3775.
27. **Morris, P. D., A. K. Byrd, A. J. Tackett, C. E. Cameron, P. Tanega, R. Ott, E. Fanning, and K. D. Raney.** 2002. Hepatitis C virus NS3 and simian virus 40 T antigen helicases displace streptavidin from 5′-biotinylated oligonucleotides but not from 3′-biotinylated oligonucleotides: evidence for directional bias in translocation on single-stranded DNA. Biochemistry **41:**2372–2378.
28. **Neumann, A. U., N. P. Lam, H. Dahari, M. Davidian, T. E. Wiley, B. P. Mika, A. S. Perelson, and T. J. Layden.** 2000. Differences in viral dynamics between genotypes 1 and 2 of hepatitis C virus. J. Infect. Dis. **182:**28–35.
29. **Pang, P. S., E. Jankowsky, P. J. Planet, and A. M. Pyle.** 2002. The hepatitis C viral NS3 protein is a processive DNA helicase with cofactor enhanced RNA unwinding. EMBO J. **21:**1168–1176.
30. **Paolini, C., R. De Francesco, and P. Gallinari.** 2000. Enzymatic properties of hepatitis C virus NS3-associated helicase. J. Gen. Virol. **81:**1335–1345.
31. **Paolini, C., A. Lahm, R. De Francesco, and P. Gallinari.** 2000. Mutational analysis of hepatitis C virus NS3-associated helicase. J. Gen. Virol. **81:**1649–1658.
32. **Porter, D. J. T., S. A. Short, M. H. Hanlon, F. Preugschat, J. E. Wilson, D. H. Willard, Jr., and T. G. Consler.** 1998. Product release is the major contributor to k_{cat} for the hepatitis C virus helicase-catalyzed strand separation of short duplex DNA. J. Biol. Chem. **273:**18906–18914.
33. **Preugschat, F., D. R. Averett, B. E. Clarke, and D. J. T. Porter.** 1996. A steady-state and pre-steady-state kinetic analysis of the NTPase activity associated with the hepatitis C virus NS3 helicase domain. J. Biol. Chem. **271:**24449–24457.
34. **Preugschat, F., D. P. Danger, L. H. Carter III, R. G. Davis, and D. J. Porter.** 2000. Kinetic analysis of the effects of mutagenesis of W501 and V432 of the hepatitis C virus NS3 helicase domain on ATPase and strand-separating activity. Biochemistry **39:**5174–5183.
35. **Suzich, J. A., J. K. Tamura, F. Palmer-Hill, P. Warrener, A. Grakoui, C. M. Rice, S. M. Feinstone, and M. S. Collett.** 1993. Hepatitis C virus NS3 protein polynucleotide-stimulated nucleoside triphosphatase and comparison with the related pestivirus and flavivirus enzymes. J. Virol. **67:**6152–6158.
36. **Tai, C.-L., W.-K. Chi, D.-S. Chen, and L.-H. Hwang.** 1996. The helicase activity associated with hepatitis C virus nonstructural protein 3 (NS3). J. Virol. **70:**8477–8484.
37. **Tai, C.-L., W.-C. Pan, S.-H. Liaw, U.-C. Yang, L.-H. Hwang, and D.-S. Chen.** 2001. Structure-based mutational analysis of the hepatitis C virus NS3 helicase. J. Virol. **75:**8289–8297.
38. **Taylor, D. R., S. T. Shi, P. R. Romano, G. N. Barber, and M. M. Lai.** 1999. Inhibition of the interferon-inducible protein kinase PKR by HCV E2 protein. Science **285:**107–110.
39. **Wang, H., T. Bian, S. J. Merrill, and D. D. Eckels.** 2002. Sequence variation in the gene encoding the nonstructural 3 protein of hepatitis C virus: evidence for immune selection. J. Mol. Evol. **54:**465–473.
40. **Weiner, A., A. L. Erickson, J. Kansopon, K. Crawford, E. Muchmore, A. L. Hughes, M. Houghton, and C. M. Walker.** 1995. Persistent hepatitis C virus infection in a chimpanzee is associated with emergence of a cytotoxic T lymphocyte escape variant. Proc. Natl. Acad. Sci. USA **92:**2755–2759.
41. **Yanagi, M., R. H. Purcell, S. U. Emerson, and J. Bukh.** 1999. Hepatitis C virus: an infectious molecular clone of a second major genotype (2a) and lack of viability of intertypic 1a and 2a chimeras. Virology **262:**250–263.
42. **Yanagi, M., R. H. Purcell, S. U. Emerson, and J. Bukh.** 1997. Transcripts from a single full-length cDNA clone of hepatitis C virus are infectious when directly transfected into the liver of a chimpanzee. Proc. Natl. Acad. Sci. USA **94:**8738–8743.
43. **Yanagi, M., M. St. Claire, M. Shapiro, S. U. Emerson, R. H. Purcell, and J. Bukh.** 1998. Transcripts of a chimeric cDNA clone of hepatitis C virus genotype 1b are infectious in vivo. Virology **244:**161–172.
44. **Yao, N., T. Hesson, M. Cable, Z. Hong, A. D. Kwong, H. V. Le, and P. C. Weber.** 1997. Structure of the hepatitis C virus RNA helicase domain. Nat. Struct. Biol. **4:**463–467.
45. **Zein, N. N.** 2000. Clinical significance of hepatitis C virus genotypes. Clin. Microbiol. Rev. **13:**223–235.